Magneto-optical study of the spin-polarized electronic states in multiferroic TbMnO₃

M. Bastjan,[1] S. G. Singer,[1] G. Neuber,[1] S. Eller,[1] N. Aliouane,[2] D. N. Argyriou,[2] S. L. Cooper,[3] and M. Rübhausen[1]

[1]*Institut für Angewandte Physik, Universität Hamburg, Jungiusstraße 11, D-20355 Hamburg, Germany*

[2]*Hahn-Meitner Institut, Glienicker Straße 100, D-14109 Berlin, Germany*

[3]*Frederick Seitz Materials Research Laboratory and Department of Physics, University of Illinois at Urbana-Champaign, Urbana, Illinois 61801, USA*

The magnetic and electronic properties of multiferroic TbMnO₃ in the paramagnetic, antiferromagnetic, sinusoidal, and spiral-spin phases were studied by spectral generalized magneto-optical ellipsometry. The measurements show a strong anisotropy of the dielectric tensor. A redistribution of spectral weight was observed in the diagonal components of the dielectric tensor for the temperature range from 110 to T_N=46 K. In the off-diagonal elements, spectral generalized magneto-optical ellipsometry shows sensitivity to the antiferromagnetic and ferroelectric phase transitions at T_N=46 K and T_F=29 K, respectively, and a persistent signal up to $6T_N$.

Multiferroic materials exhibit phases with simultaneous magnetic and ferroelectric properties. The close coupling of the magnetization and the electric polarization in multiferroics makes these materials excellent candidates for demonstrating giant magnetoelectrical behavior,[1,2] in which large magnetic and electric responses can be induced with weak electric and magnetic fields, respectively.[3,4] Spectral generalized magneto-optical ellipsometry (SGME) is an ideal technique for studying the interplay between electric and magnetic properties in multiferroic systems, as it probes both the diagonal ε_{xx} and off-diagonal ε_{xy} components of the dielectric tensor.[5]

Multiferroicity in TbMnO₃ is induced by spin-charge coupling. Below the Néel temperature T_N=46 K, the wavelength of the incommensurate spin density decreases with decreasing temperature down to the ferroelectric transition at T_F=29 K. In the absence of a magnetic field, this spin-density modulation gets locked in at T_F. Below T_F, the inversion symmetry of the lattice is broken by the bc-cycloidal arrangement of the spins, inducing a ferroelectric polarization along the c axis while the antiferromagnetic ordering along the b axis persists.[3,4,6]

Here, we study the coupling between spin and charge degrees of freedom in multiferroic TbMnO₃ by examining the temperature-dependent dielectric responses ε_{xx} and ε_{xy}, which are the diagonal and off-diagonal components of the dielectric tensor. The magnetization of a material breaks the symmetry between left and right circularly polarized (LCP and RCP) light. While ε_{2xx} is proportional to the sum of absorptions of LCP and RCP light, ε_{1xy} is proportional to the difference.[7] Consequently, a complete magneto-optical characterization of ε_{2xx} and ε_{1xy} in a magnetic material provides detailed information regarding the coupling between the material's electronic and magnetic properties.

The temperature-dependent ellipsometry was done with a custom-made setup by using an extended Sentech SE850 spectral ellipsometer inside a He flow cryostat. The cryostat has stress-free mounted windows and maintains a base pressure of about 3×10^{-8} mbar at room temperature.[8] Standard ellipsometry was performed for temperatures from 10 to 470 K in the spectral range from 0.5 to 5.5 eV. In SGME, one measures the fractional difference of the intensities of light at a particular polarization angle for magnetic fields, which is applied along opposite directions, i.e., $\delta I / I = 2(I_\downarrow - I_\uparrow)/(I_\downarrow + I_\uparrow)$.[8,9] A magnetic field $H = \pm 440$ mT was applied parallel to the normal vector of the plane of incidence. SGME measurements were performed in the spectral range from 1.6 to 5.5 eV for temperatures from 15 to 300 K. For measurements on the BC plane, two identical lenses were mounted in order to reduce the spot size to 100×300 μm².

The TbMnO₃ crystals were grown at the Hahn-Meitner Institut in a floating zone image furnace under Ar atmosphere. The phase purity of these crystals was checked by performing x-ray and neutron diffraction measurements on a small part of each sample. The resulting diffraction patterns indicate that the samples were single phase and orthorhombic. The specific heat and superconducting quantum interference device (SQUID) measurements show three successive transitions at T_N(Mn)=46 K, T_F=29 K, and T_N(Tb)=7 K, which are in good agreement with published data.[2] The TbMnO₃ samples have dimensions of $6 \times 5 \times 2$ and $5 \times 3 \times 2$ mm³. They were polished on an exposed AB and BC planes.

In Figs. 1(a) and 1(c), we present the real (ε_{1xx}) and imaginary (ε_{2xx}) parts of the diagonal elements of the dielectric tensor of TbMnO₃. The quantity ε^c denotes the dielectric function in the c-axis direction. For both planes, the temperature range between 10 and 450 K was investigated. The spectra for the BC plane were taken along the c axis [Fig. 1(c)] and a direction 17° off the b axis [Fig. 1(a)]. Figure 1(b) shows ε_{1xx} and ε_{2xx} on the AB plane along a direction 25° off the b axis, for the same temperatures. While the measurements close to the b axis, on both planes, show bands centered around 2 and 5 eV [Figs. 1(a) and 1(b)], only the 5 eV band is present for ε^c_{xx} [Fig. 1(c)]. The band at 2 eV exhibits an anisotropy and a temperature dependence. The origin of the 2 eV band in undoped manganites has been studied by several authors.[10–15] In more detail, the 2 eV band consists of three separate peaks at roughly 1.9, 2.3, and 2.6 eV. At low temperatures, for measurements on the AB
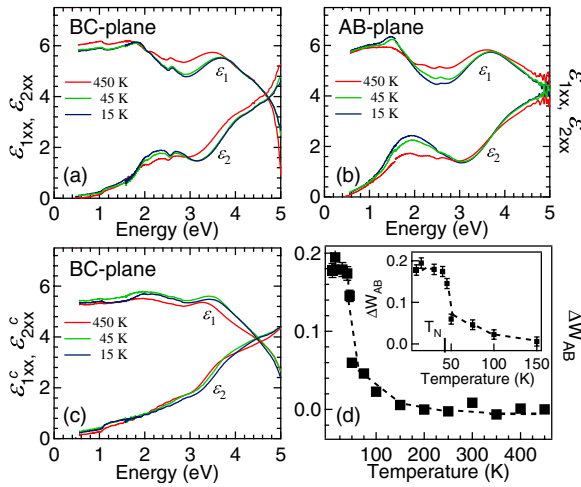
FIG. 1. (Color online) Diagonal elements (ε_{xx}) of the dielectric tensor of TbMnO$_3$ for 450 (red), 45 (green), and 15 K (blue), which are measured on the BC [(a) and (c)] as well as on the AB plane [see (b)]. The ε_{1xx} and ε_{2xx} are the real and the imaginary parts of the dielectric function. (d) shows the changes in the normalized integrated spectral weight as a function of temperature for the AB plane. The inset displays details of these changes in temperatures between 10 and 150 K.

plane close to the b axis, the appearance of three separate peaks is less pronounced [see Fig. 1(b)]. In recent publications, Kovaleva *et al.*[13] and Kim *et al.*[14,15] assigned this 2 eV band to intersite Mn^{3+} d-d transitions. In contrast, the band at 5 eV is mainly isotropic and can be associated with the manifold of charge transfer transitions from O $2p \rightarrow$ Mn $3d$ levels starting around 3 eV and extending to much higher energies.[16]

The number of charge carriers is commonly conserved across a phase transition and its density is connected to the integrated optical conductivity $\sigma_{xx} = \sigma_{1xx} + i\sigma_{2xx}$. In turn, the diagonal element of the dielectric function ε_{xx} is directly related to $\sigma_{xx}(\omega) \propto i\omega\varepsilon_{xx}(\omega)$. Hence, a good quantity to study the temperature dependence of the charge density is the normalized integrated spectral weight difference,

$$\Delta W(T) = \frac{\int_{\omega_1}^{\omega_2}[\sigma_{1xx}(\omega, T) - \sigma_{1xx}(\omega, T_{\text{ref}})]d\omega}{\int_{\omega_1}^{\omega_2}\sigma_{1xx}(\omega, T_{\text{ref}})d\omega}, \qquad (1)$$

with $T_{\text{ref}} = 450$ K. This quantity should vanish in the case of a conservation of the carrier density inside the observed spectral range. Figure 1(d) shows the development of $\Delta W(T)$ for the AB plane, which is integrated over the spectral range from $\omega_1 = 0.5$ eV to $\omega_2 = 4.5$ eV. The spectral weight is conserved in the investigated spectral range for temperatures between 450 and 110 K. However, below 110 K, an increase in $\Delta W(T)$ is visible. According to Eq. (1), this implies a shift of spectral weight into the observed spectral range for temperatures below 110 K. This spectral weight presumably comes from higher energies as the low energy response remains marginal.[16] Below 40 K, the spectral weight is constant as can be seen more clearly in the inset of Fig. 1(d).

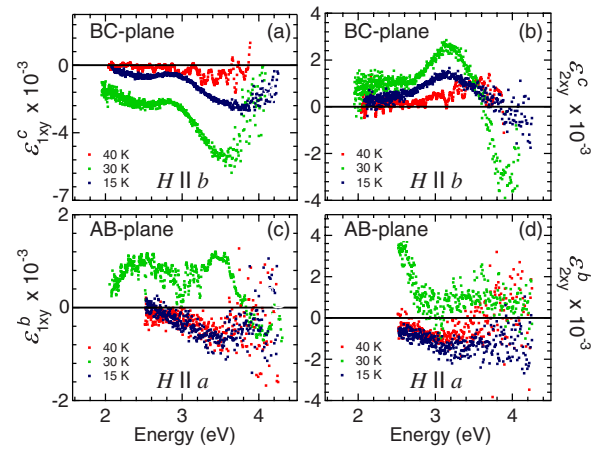In order to connect the results of the spectral weight trans-

fers, as shown in Fig. 1(d), with the development of the magnetic order, we have correlated these data with the temperature dependence of the off-diagonal components ε_{xy} of the dielectric tensor, which gives information about the spin polarization of the electronic states.

Figure 2 presents ε_{xy} for three temperatures: 40, 30, and 15 K, which are close to T_N, T_F, and below T_F, respectively. Figure 2 shows both the real part ε_{1xy} (left panel) and the imaginary part ε_{2xy} (right panel). The largest temperature-dependent changes were observed for measurements on the BC plane along the c axis, with $H \| b$ [Figs. 2(a) and 2(b)]. In this geometry, a peak in ε_{2xy} is observed around 3.2 eV; this peak is strongest at 30 K, but is also present at 15 K. Measurements on the AB plane were also performed for measurements along the b axis with $H \| a$, but the intensity is much weaker [Figs. 2(c) and 2(d)].

For a better understanding of our data, we present a sketch of the spin orientations, with and without an applied magnetic field H [Fig. 3]. For measurements on the BC plane, the sinusoidal (spiral) J_{SS} and antiferromagnetic J_{AF} spin coupling are both present. Along the a axis, the ferromagnetic spin coupling J_{FM} exists. By applying an external magnetic field $H \| b$, we expect a net magnetic moment along

FIG. 2. (Color online) The real (ε_{1xy}) and imaginary (ε_{2xy}) part of the off-diagonal elements of the dielectric tensor for 15 (blue), 30 (green), and 40 (red) of TbMnO$_3$.
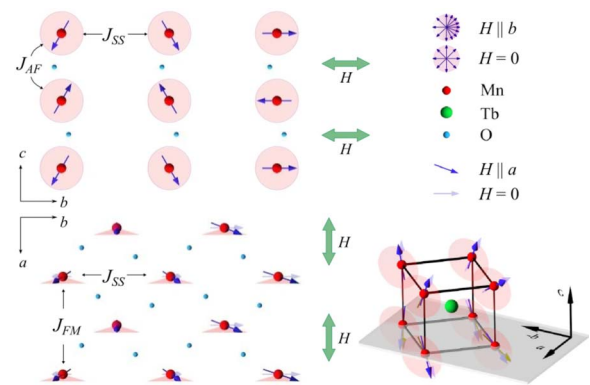

FIG. 3. (Color online) Sketch of the spin orientations for the examined planes. J_{SS} describes the sinusoidal and spiral, J_{AF} the antiferromagnetic, and J_{FM} the ferromagnetic spin couplings.
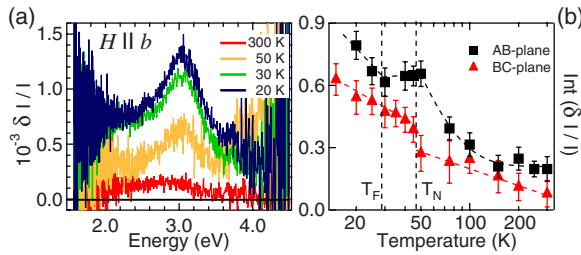
FIG. 4. (Color online) (a) Temperature dependence of the fractional intensity change $\delta I/I$ measured for $H=440$ mT, which is polarizer position $-30°$ and analyzer position $10°$. (b) Integrated $\delta I/I$ spectra between 1.75 and 4.0 eV as a function of temperature.

the b axis, as illustrated in the top right picture in Fig. 3. The off-diagonal components of the dielectric tensor ε are calculated from many $\delta I/I$ measurements for different polarizer and analyzer orientations.[8] Thus, $\delta I/I$ shows a similar temperature dependence for both planes [Fig. 4].

Figure 4(a) shows the fractional intensity changes $\delta I/I$ as a function of energy, for different temperatures, taken on the BC plane along the c axis and for $H \| b$. For all measurements, the same polarizer orientation $\theta_1 = -30°$ and analyzer orientation $\theta_2 = +10°$ were kept.

These spectra display a peak centered around 3.0 eV, which present for all measurements even above $6T_N$. In Fig. 4(b), the corresponding integrals of each $\delta I/I$ spectrum ($\omega \in [1.75, 4.0]$ eV) are shown as a function of temperature for both planes. For measurements on the BC plane (red triangles), the integrated weight between 1.75 and 4.0 eV linearly increases with decreasing temperature but exhibits an abrupt increase at $T_N = 46$ K. For measurements on the AB plane (black squares), a stronger, nonlinear increase in the integrated weight is observed down to T_N, followed by a constant integrated weight between T_N and T_F. At temperatures below T_F, at which a spiral-spin-modulation is present in TbMnO$_3$,[6] our measurements on the AB-plane indicate a systematic increase in the integrated weight. This shows that

the off-diagonal components of the dielectric function with $H \| b$ are quite sensitive to the transition into the ferroelectric state, which is in contrast to the diagonal components, which show no sensitivity to the ferroelectric transition [Fig. 1(d)].

With the help of Fig. 3 and the interpretation of the $\delta I/I$ spectra (Fig. 4), we explain the differences between the off-diagonal components for the AB and BC planes [Fig. 2]. For both planes, due to the applied magnetic field H, a shift of the spin density in the spiral and sinusoidal phase is present. For the AB plane, a tilt of the spins out of their rotating direction by an external field H exists, but due to the different couplings (J_{FM}, J_{SS}, and J_{AF}) along the corresponding axis, the signals are of different strength. The second phase transition at $T_F = 29$ K was only observable for the AB plane [Fig. 4(b)]. In principle, the sinusoidal modulation misses a component parallel to the a axis, which explains why this phase transition is not apparent in the BC projection. Due to the pure magnetic coupling, the sinusoidal spiral transition is not observable in standard ellipsometry (see Fig. 1). We would like to emphasize that our interpretation does not rely on the Dzyaloshinski–Moriya interaction, which may induce a persistent ferromagnetic moment along the c axis.[17,18]

By combining standard spectral and magneto-optical ellipsometry, we have studied the charge and spin polarizations of multiferroic TbMnO$_3$. The magneto-optical measurements show changes in the electronic structure for temperatures below T_N and T_F. Furthermore, our data exhibit a sensitivity to the sinusoidal spiral phase transition. The observation of a signal up to 300 K (approximately $6T_N$) is consistent with the formation of short range magnetic ordering well above T_N.

[1] M. Fiebieg, J. Phys. D **38**, R123 (2005).

[2] T. Kimura, T. Goto, H. Shintani, K. Ishizaka, T. Arima, and Y. Tokura, Nature (London) **55**, 426 (2003).

[3] M. Kenzelmann, A. B. Harris, S. Jonas, C. Broholm, J. Schefer, S. B. Kim, C. L. Zhang, S.-W. Cheong, O. P. Vajk, and J. W. Lynn, Phys. Rev. Lett. **95**, 087206 (2005).

[4] M. Mostovoy, Phys. Rev. Lett. **96**, 067601 (2006).

[5] R. Rauer, M. Rübhausen, and K. M. Dörr, Phys. Rev. B **73**, 092402 (2006).

[6] N. Aliouane, D. N. Argyriou, J. Strempfer, I. Zegkinoglou, S. Landsgesell, and M. V. Zimmermann, Phys. Rev. B **73**, 020102(R) (2006).

[7] H. S. Bennet and E. A. Stern, Phys. Rev. **137**, A448 (1965).

[8] R. Rauer, G. Neuber, J. Kunze, J. Bäckström, and M. Rübhausen, Rev. Sci. Instrum. **76**, 023910 (2005).

[9] A. Berger and M. R. Pufall, Appl. Phys. Lett. **71**, 965 (1997).

[10] V. Perebeinos and P. B. Allen, Phys. Rev. Lett. **85**, 5178 (2000).

[11] K. Tobe, T. Kimura Y. Okimoto, and Y. Tokura, Phys. Rev. B **64**, 184421 (2001).

[12] R. Krüger, B. Schulz, S. Naler, R. Rauer, D. Budelmann, J. Bäckström, K. H. Kim, S.-W. Cheong, V. Perebeinos, and M. Rübhausen, Phys. Rev. Lett. **92**, 097203 (2004).

[13] N. N. Kovaleva, A. V. Boris, C. Bernhard, A. Kulakov, A. Pimenov, A. M. Balbashov, G. Khaliullin, and B. Keimer, Phys. Rev. Lett. **93**, 147204 (2004).

[14] M. W. Kim, P. Murugavel, Sachin Parashar, J. S. Lee, and T. W. Noh, New J. Phys. **6**, 156 (2004).

[15] M. W. Kim, S. J. Moon, J. H. Jung, Jaejun Yu, Sachin Parashar, P. Murugavel, J. H. Lee, and T. W. Noh, Phys. Rev. Lett. **96**, 247205 (2006).

[16] A. Rusydi, R. Rauer, G. Neuber, M. Bastjan, I. Mahns, S. Müller, P. Saichu, B. Schulz, S. G. Singer, A. I. Lichtenstein, G. Stryganyuk, K. Dörr, G. A. Sawatzky, S. L. Cooper, and M. Rübhausen, Phys. Rev. Lett. (to be published).

[17] I. Dzyaloshinskii, J. Phys. Chem. Solids **4**, 241 (1958).

[18] T. Moriya, Phys. Rev. **120**, 9 (1960).